ScienceDirect

Journals & Books

Create account

Sign in

Brought to you by:
B-on Consortium of Portugal

Download   Share   Export

Alkali-activated binary mortar based on natural volcanic pozzolan for repair applications

Rafael Robayo-Salazar [a], Carlos Jesús [b], Ruby Mejía de Gutiérrez [a] ✉, F. Pacheco-Torgal [b]

⊞ Show more

Get rights and content

Highlights

- Alkali-activated binary mortar (AABM) was obtaining and physico-mechanical characterized.

- The adherence (pull-off) of the AABM to three substrate class (OPC concretes) was evaluate.

- The adherence (pull-off) obtained varied between 0.75 and 1.24 MPa.

- The strength class of the substrate promoted the greatest pull-off adhesions.

- AABM was classified as a "class R2–repair mortar" according to EN 1504-3.

Abstract

The goal of this investigation was evaluate the potential of an alkali-activated binary mortar (AABM), based on a natural volcanic pozzolan (70%) and granulated blast furnace slag (30%), as a repair material. This evaluation focused on its physico-mechanical characterisation (compressive, flexural and splitting tensile strengths; modulus of elasticity; capillary water absorption; and shrinkage) and the measurement of its adherence to three class of OPC concretes (substrates) using pull-off tests. A mixture of NaOH and Na_2SiO_3 was used as alkaline activator. The compressive and splitting tensile strength of AABM were 34.8 MPa and 2.13 MPa at 28 days of curing, respectively. Its capillary absorption coefficient and modulus of elasticity were 0.5088 kg/m^{2}h$^{0.5}$ and 8.66 GPa respectively. The results of the pull-off test demonstrate the adherent nature of the AABM, which was promoted by the strength (quality) of the OPC substrate, with pull-off adherences of 0.75 MPa, 1.14 MPa and 1.24 MPa for class C25/30, C35/45 and C50/60, respectively. According to the results obtained and standard specifications (EN 1504-3), this material can be classified as a class R2-repair mortar.

Keywords

Alkali-activated materials; Coating mortar; Repair mortar; Pull-off; Natural volcanic pozzolan

1. Introduction

Surface deterioration, spalling, seepage, cracking and other common damage to infrastructure based on ordinary Portland cement (OPC) concrete are a continuous cause of concern worldwide due to the high costs associated to the protection, repair and rehabilitation of these pathologies with commonly employed materials [1,2]. The recurrence or repetitive appearance of this pathologies prompts the search for alternative solutions and highlights the use of *alkali-activated materials* (AAM) as materials with high potential application in this field [[3], [4],

[5], [6], [7]]. In addition, AAM are considered to be materials with low carbon footprints (CO_2); their use in these types of applications can contribute to the future sustainability of the construction industry [3,[8], [9], [10]].

AAM are binders that are produced by the chemical interaction between an aluminosilicate (precursor), which can have a natural (volcanic pozzolans) or artificial origin, and a strongly alkaline solution [[11], [12], [13], [14], [15], [16], [17]]. This chemical interaction, which occurs at relatively low processing temperatures (≤90 °C), promote the obtaining reaction products of high-strength and durability via dissolution, condensation and precipitation processes [18,19]. The calcium content, which is originally present in the precursor or added by a secondary source, has an important role in the kinetics of these reactions and the development of adequate mechanical performance at room temperature and promotes the precipitation of calcium silicate hydrated (C-S-H), calcium aluminosilicate hydrated (C-A-S-H) and/or calcium-sodium aluminosilicate hydrated ((C,N)-A-S-H), in addition to the precipitation of sodium aluminosilicate hydrated (N-A-S-H) gel [[20], [21], [22], [23]]. This compositional factor is important because the curing at room temperature is mandatory for *in situ* applications, such as the protection, repair or rehabilitation of concrete structures.

The mechanical performance of AAM at room temperature is also influenced by the precursor reactivity (amorphous), size of particles and the optimisation of synthesis conditions; including the type and/or concentration of the alkaline activator [[24], [25], [26], [27]]. The hardening and strength development at early ages are considered advantages in the field of *rapid-repair materials*, which are commonly employed in *patch repair* applications that demand an almost instantaneous adherence to the substrate [1,6,28]. The main characteristic that drives the use of AAM in the field of protection (coatings) and repair of structures based on OPC concrete is their adherent nature [2,3,29], which is favoured by the presence of silicate alkaline activators (Na_2SiO_3 or K_2SiO_3). In this regard, the European Standard EN1504-3 [30] recommends that the minimum adherence (pull-off) between the repair material and the substrate (OPC) must be 0.8 MPa. Some authors [[31], [32], [33], [34], [35]] have evaluated the AAM adherence to the OPC concrete by slant shear and direct shear tests; the results are generally satisfactory [3,4]. It should be noted that reports of pull-off test of alkali-activated materials on OPC substrates are scarce.

In addition to their adherent nature, different authors describe AAM as materials with a higher chemical resistance (durability) than the chemical resistance of OPC concrete [[36], [37], [38]]. They attribute this performance to the type of porosity (meso- and micro-porosity), the three-dimensional micro-structure and nature of the reaction products (gels) that are obtained via alkaline activation [[39], [40], [41]]. The possibility of increasing the durability (or service life) of OPC concrete by the use of AAM protective coatings is an important alternative for this industry [28,[42], [43], [44], [45]], especially in the field of reinforced structures that are exposed to aggressive environments that are susceptible to accelerated deterioration and corrosion phenomena [[46], [47], [48], [49], [50], [51]].

The European EN 1504 standard [30] specifies the requirements for the classification of products and systems that will be employed for the structural and non-structural protection or repair of reinforced concrete. Part 3 of this standard addresses repair mortars and concretes that can be used in conjunction with other products and systems to restore and/or replace defective or contaminated concrete and protect the reinforcement to extend the service life of a concrete structure that has deteriorated. According to the EN 1504-3 standard, the compatibility between the coating material and the substrate is related to properties such as adhesion (pull-off), capillary absorption (water permeability), shrinkage, compressive strength and modulus of elasticity and factors associated with the durability and the application method. The EN 1504-3 defines four classes of repair products (structural (class R3 and class R4)) and non-structural (class R1 and class R2) based on these physico-mechanical characteristics and their level of adherence (pull-off) to the substrate.

The goal of this investigation was to obtain an alkali-activated binary mortar (AABM) and evaluate its potential as a protection or repair material by focusing on its physico-mechanical characterisation (capillary water absorption; shrinkage; compressive, flexural and splitting tensile strengths; and modulus of elasticity) and the measurement of its adherence to three types of OPC concretes (substrates) using pull-off tests. The results are applied to its classification according to the EN 1504-3 standard [30].

## 2. Materials and methodology

2.1. Materials

As precursor (aluminosilicate), a binary mixture composed of a Colombian natural volcanic pozzolan (NP) (70%) and granulated blast furnace slag (GBFS) (30%) was employed. The mean particle sizes of the NP and GBFS, which were determined by laser granulometry, were 21 μm and 26 μm, respectively. The chemical compositions of these materials, which is determined by X-ray fluorescence, are listed in Table 1. Fig. 1 shows the pattern of X-ray diffraction of the precursors (NP and GBFS). The amorphous phase content of the NP was determined by Rietveld X-ray diffraction (XRD) refinement following the methodology proposed by De La Torre et al. [52] and using a corundum (Al_2O_3) standard. The results of the quantitative analysis yielded an amorphous phase content of 25.5%. According to the mineralogical analysis through X'Pert HighScore Plus software, the crystalline fraction of NP is mainly composed by sodium-calcium feldspars or plagioclase structures (albite-anorthite series, 59.3%) in addition to some minerals that belong to the amphibole group (10.4%) and quartz (4.8%). The GBFS XRD reflects its vitreous nature (halo located in the range between 23° and 37° 2θ). Signals that correspond to crystalline structures associated with gehlenite ($2 \cdot CaO \cdot Al_2O_3 \cdot SiO_2$) and calcite ($CaCO_3$) are observed.

Table 1. Chemical composition of the NP and GBFS used as precursors (wt % of oxides).

Material	SiO$_2$	Al$_2$O$_3$	Fe$_2$O$_3$	CaO	Na$_2$O	MgO	K$_2$O	LOI[a]	Others	SiO$_2$/Al$_2$O$_3$ (Molar)
NP	61.99	15.52	7.33	5.19	4.07	2.49	1.59	0.48	1.34	6.79
GBFS	37.74	15.69	1.85	40.30	0.20	1.30	0.40	–	2.52	4.09

[a]
LOI: Loss on ignition.
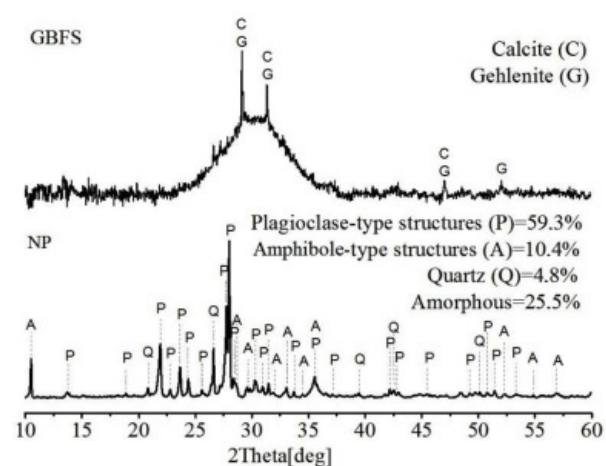
Fig. 1. XRD analysis of the precursors (NP and GBFS).

The use of NP in the alkaline activation is considered to be an alternative that guarantees sustainable production on an industrial scale for this type of material due to its availability and global distribution [53]. However, due to its predominant semi-crystalline nature and its deficiencies in CaO and reactive Al$_2$O$_3$ contents, it is necessary to apply thermal curing (60–90 °C) in order to promote the mechanical performance of these materials at early curing ages [54]. The addition of GBFS as a calcium source, in low proportions (up to 30%), favours the development of adequate mechanical performance at room temperature, required for *in situ* applications such as protection and repair of concrete structures, promoting the formation of calcium silicate hydrated (C-S-H) and calcium aluminosilicate hydrated (C-A-S-H) [[55], [56], [57]].

A blend of NaOH pellets (industrial grade), commercial sodium silicate Na$_2$SiO$_3$ (58.7% SiO$_2$, 13.5% Na$_2$O, 45.2% H$_2$O) and tap water, to achieve a molar ratio SiO$_2$/Na$_2$O=1.1, was employed as alkaline activator [57]. To obtain the AABM, a natural sand which fineness modulus of 2.5 was employed.

To produce substrates based on OPC (concretes), the same sand and crushed gravel with a maximum size of 19.05 mm was employed. The type of OPC used in the production of the substrates was CEM I 42.5 R.

2.2. Mixtures design

The synthesis of the *alkali-activated binary binder* (AABB), which is the base material for obtaining the mortar (AABM), was performed based on the optimum conditions (content of alkaline activator and % of GBFS) defined in a previous study [57]. The dosage per cubic metre of the AABM is listed in Table 2. For its proportioning, a precursor:sand ratio (in weight) of 1:2.75 was established. The liquid/solids ratios (L/S) for pastes (AABB) and mortars (AABM) were 0.20 and 0.35, respectively.

Table 2. Dosage (kg) per cubic metre (m^3) of alkali activated binary mortar (AABM) (coating mortar).

Material	NP	GBFS	Water	NaOH	Na$_2$SiO$_3$	Sand
kg/m^3	363.0	155.6	138.4	36.5	172.6	1426.0

Prior to the mixing process, a dry homogenisation of the precursors (70%NP+30%GBFS) was performed. The mixtures were obtained in a Controls L5 automatic mixer with a total mixing time of 5 min; a constant low speed (spindle speed 115 r.p.m.) was maintained for the entire duration of the mixing. The mixing process of the AABM was realized during 5 min, first was added the alkaline activator and after was incorporated the sand. The mixtures were moulded and vibrated for 30 s to release the air trapped during the mixing process. After

24 h, the specimens were demoulded and cured in laboratory conditions (20 ± 3 °C and 70 ± 10% of room temperature and relative humidity, respectively) until the test age was attained.

2.3. Experimental tests

The microstructural characterisation of the binder (AABB) was based on the complementary techniques XRD and energy dispersive spectroscopy-scanning electron microscopy (EDS-SEM).

The compressive strength was obtained in a LLOYD LR50K universal press by testing 50.8 mm cube specimens for mortars (AABM) (ASTM C109 [58]) and 20 mm cube specimens for pastes (AABB). The determination of the secant elastic modulus in compression (EN 12390-13 [59]) of the AABM (28 days) was performed using cylinders with a diameter of 60 mm (height to diameter ratio = 2). The three-point flexural strength (ASTM C348 [60]) of the AABM (28 days) was obtained in 40 mm × 40 mm x 160 mm beams. The splitting tensile strength of the AABM was evaluated at 28 days in cylinders with a diameter of 60 mm (height to diameter ratio = 2) by adapting the procedure described in the ASTM C496 standard [61].

The water absorption coefficient (capillarity) of the AABM was determined at 28 days of curing based on the EN 1015-18 standard [62]. For the measurement of the shrinkage, 40 mm × 40 mm x 160 mm beams were used. The procedure for the evaluation of the length change followed the recommendations of the ASTM C490 standard [63]. For this test, the measurements were recorded once the beams hardened and could be demoulded (≈2 h for the AABM and 24 h for the reference material (OPC substrate)) and continued until 28 days of curing. The specimens were kept in laboratory conditions (20 ± 3 °C and 70 ± 10% of relative humidity) during the entire test. To record the length change, a Mahr-MarCator 1075 R digital device was employed (accuracy of gauge ± 0.001).

The values reported in each of the physico-mechanical tests correspond to an average of three specimens per mixture and/or test age.

2.4. OPC concrete substrates

To evaluate the effect of the substrate quality on the adherence (pull-off) of the AABM, three types of OPC concretes (substrates) were obtained. The proportioning of these concretes, which are presented in Table 3, was based on obtaining three strength classes (EN 206-1 [64]): C25/30, C35/45 and C50/60. These mixtures were obtained in a horizontal mixer with a total mixing time of 8 min. According to the EN 1542 standard [65], the mixtures were moulded into 300 mm × 300 mm x 100 mm plates, vibrated for 30 s to remove the air trapped during the mixing process, and subsequently cured for 28 days in immersion (under water). The control of this strength was performed at 28 days of curing in a 3000 KN capacity ELE hydraulic press, for which 100 mm cubes were employed (EN 12390 [59]). The compressive strength (28 days of curing) for C25/30, C35/45 and C50/60 was 36.2, 50.3 and 64.9 MPa, respectively.

Table 3. Dosage (kg) per cubic metre (m^3) and characterisation of OPC concrete substrates.

Material Proportions (kg/m^3)	Concrete class EN 206-1		
	C 25/30	C 35/45	C 50/60
Portland cement (OPC)	350.0	450.0	550.0
Water	157.5	180.0	192.5
Sand	1075.5	1002.0	934.5
Gravel	717.0	668.0	623.0
Superplasticiser	5.3	6.8	8.3
Properties			
Slump class (EN 12350-2)	S2	S2	S3
C.S. (MPa) (EN 12390)	36.2 ± 2.4	50.3 ± 2.3	64.9 ± 1.7

C.S. = compressive strength (28 days of curing).

2.5. Surface preparation of concrete substrates, application of coating mortar and pull-off test

The OPC substrates (C25/30, C35/45 and C50/60) in the pull-off test correspond to 300 mm × 300 mm x 100 mm plates (Fig. 2a). After 28 days of curing (under water), the plates were air-dried for seven days, and the upper surface was subsequently prepared by sand-blasting (Fig. 2b), according to the procedure established by the EN 1542 standard [65]. After the sand-blasting procedure, the surface was characterised by the MPD laser technique (Fig. 2c) to determine the mean depth of the roughness profile (ISO 13473-1 standard [66]). The MPD laser technique enabled a mean macrotexture depth (MTD) to be established between 0.363 mm and 0.536 mm on the surface of all substrates.
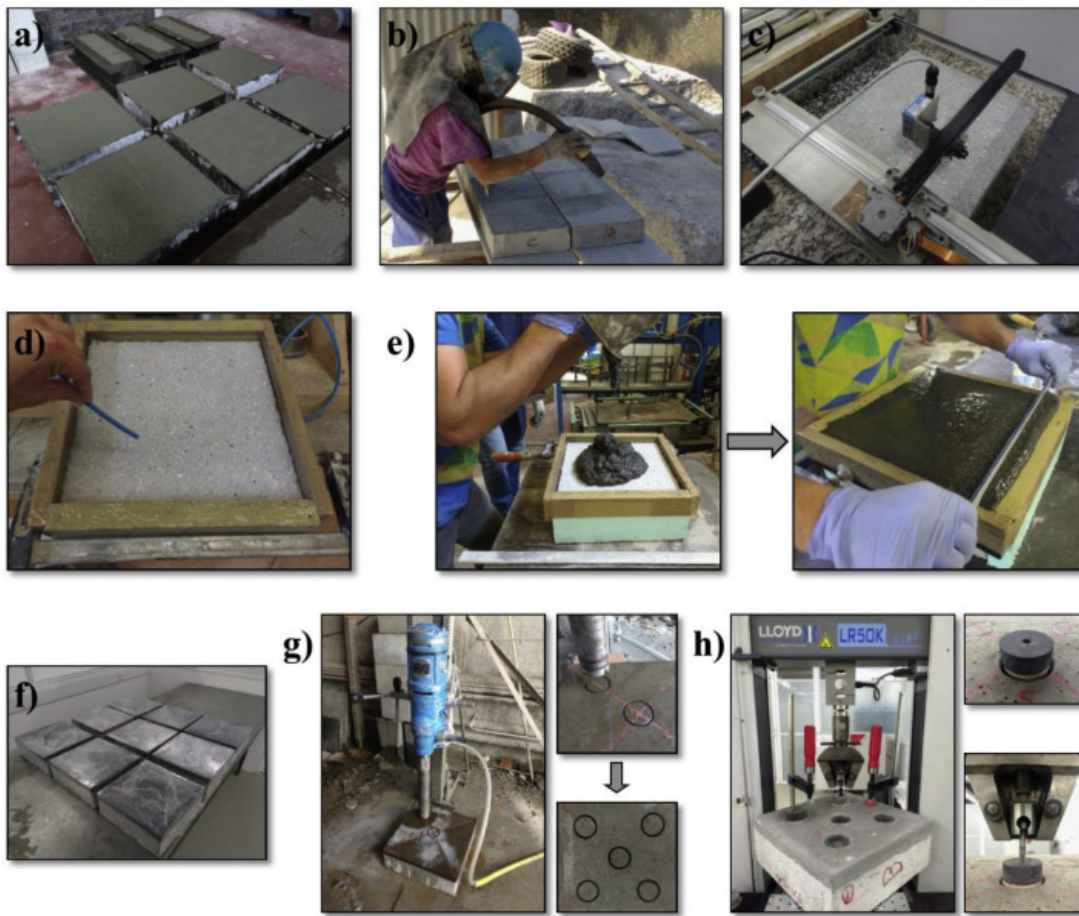
Fig. 2. Methodology used in the pull-off test (EN 1542): a) 300 mm × 300 mm ×100 mm plates (OPC substrates); b) sand-blasting process; c) surface characterisation (MPD); d) surface cleaning; e) thickness control (20 mm) of the coating; f) plate-coating systems covered with a plastic film and cured in laboratory conditions (20±3 °C and 70±10% of relative humidity) for 28 days; g) equidistant cuts with diameter of 50 mm; h) pull-out test setup and procedure.

To guarantee a coating thickness (AABM) of ≈20 mm, an adjustable frame was fixed to the plate's edges (Fig. 2d). Prior to mixing and pouring the AABM on the substrates, the surface was cleaned with pressurised air (Fig. 2d). The AABM was poured immediately after finishing the mixing process described in section 2.2; then, the mixture was distributed and compacted throughout the mould. The consistency (flow) of the AABM was between 80±5% (ASTM C1437 [67]). A final thickness of 20 mm was guaranteed by a ruler that removed the excess mixture and achieved a smooth surface of the coatings (Fig. 2e). Once the coatings hardened (≈60 min), the plate-coating systems were covered with a plastic film and cured in laboratory conditions (20±3 °C and 70±10% of relative humidity) for 28 days (Fig. 2f).

When the coatings attained a curing age of 28 days, the pull-off test was performed following the recommendations of the EN 1542 standard [65]. Previously, 50-mm-diameter circular cuts were made on the coatings, perpendicular to the surface, which penetrated 5 mm into the substrate; a total of five equidistant cuts were made per coating (Fig. 2g). A metal disk (dolly) was bound to the circular surface of each cut, which subsequently enabled the application of the tensile force during the pull-off test. A Sika Icosit® K 101 N epoxy resin was applied to bind the metal disks to the coating. The pull-off test (Fig. 2h) was performed in a LLOYD LR50K universal press, in which a tensile force was applied at a constant speed of 0.25 mm/min. For the bond stress (MPa) calculation, the ratio between the maximum pull-off load (N) and the loading area (mm^2) was considered; a total of five results per plate/coating system were obtained.

3. Results and discussion

3.1. Characterisation of alkali-activated binary binder (AABB)

Fig. 3 shows the compressive strength evolution of the alkaline binder (AABB) (paste) that was used as a base material to produce the repair mortar (AABM) compared with an OPC paste (reference or control mix) obtained in equivalent conditions. At early ages (one to seven days), the performance of the OPC paste is slightly higher than the performance of the AABB. After 28 days of curing, the opposite behaviour is observed: the AABM attains a compressive strength of 93.1 MPa at 90 days, which is 89% higher than the reported value for the OPC paste (49.3 MPa).
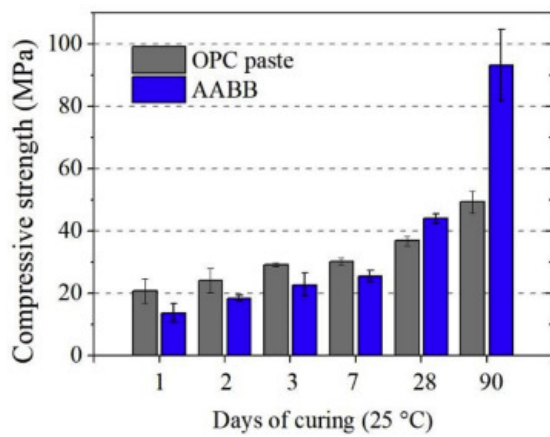
Fig. 3. Compressive strength evolution of the alkali-activated binary binder (AABB) (70%NP-30%GBFS) vs. OPC paste (cured at room temperature).

The strength evolution of the AABB to values even higher than the OPC is attributed to its micro-structure, which is enriched with the formation of (N,C)-A-S-H and/or C-(A)-S-H (high calcium compositions) reaction products over time [21,22,[68], [69], [70]]. These reaction products were identified in the AABB by a micro-structural analysis via XRD (Fig. 4a) and EDS-SEM (Fig. 4b). C-(A)-S-H type gel is predominantly amorphous, but they can form small semi-crystalline clusters such as "tobermorite" and "Jennite", that have a diffraction pattern (XRD) between 29 and 30° (2θ). Fig. 4a shows how the intensity and width of this peak increase with the addition of GBFS (30%) in the mixture. The formation of (N,C)-A-S-H and C-(A)-S-H type gels is favoured by the incorporation of GBFS in the mixture and its chemical interaction with the alkaline activator (OH⁻) [55]. This interaction causes the rupture of the bonds of its micro-structure (Ca-O; Si-O and Al-O), which supplies dissolved species (Ca^{2+}; $[H_2SiO_4]^{2-}$, $[H_3SiO_4]^-$ and $[HAlO_4]^{4-}$) that can precipitate once the maximum concentration is attained [21,68] and simultaneously generate the nucleation of these hydrates to the N-A-S-H gel (low calcium compositions) [22].
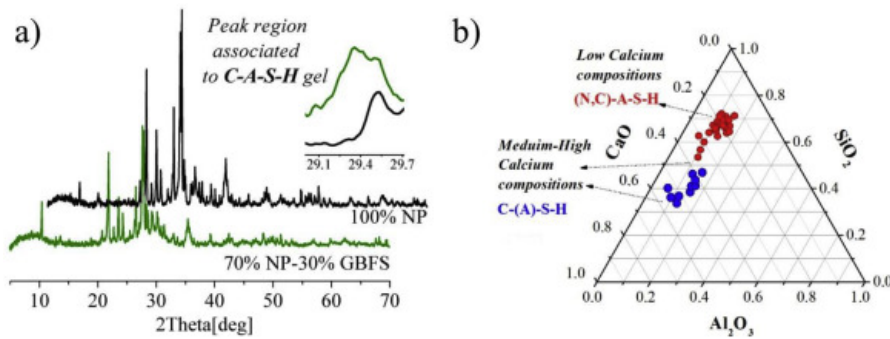
Fig. 4. Micro-structural characterisation of AABB: a) XRD (100%NP vs. 70%NP-30%GBFS) and b) $SiO_2 \cdot Al_2O_3 \cdot CaO$ ternary diagram (EDS-SEM) (70%NP-30%GBFS).

Fig. 4b shows the micro-structural composition of the 70%NP-30%GBFS mixture represented in $SiO_2 \cdot Al_2O_3 \cdot CaO$ ternary diagrams obtained from the data acquired through the EDS technique (SEM). The results are grouped in representative regions to gels type (N,C)-A-S-H (low calcium compositions) and C-A-S-H (high calcium compositions). For the mixture 70%NP-30%GBFS, the points associated with the C-A-S-H gel type, which are rich in Ca^{2+}, presented values in the range of $0.7 \le Ca/Si \le 1.8$. Theoretically, N-A-S-H gels have no Ca^{2+} presence, unlike the gel type (N,C)-A-S-H which exhibits values between $0 \le Ca/Si \le 0.4$ [[71], [72], [73], [74]]. The coexistence of these reaction products promotes a more dense and resistant structure in the AABB vs OPC, which coincides with the previously discussed results and results reported by other researchers [[55], [56], [57],75,76].

3.2. Characterisation of AABM

The characterisation of the alkaline mortar (AABM) was based on the test methods and requirements recommended by the EN 1504-3 standard [30] for structural and non-structural repair products, which are listed in Table 4.

Table 4. Main characteristics and/or requirements of the repair products (structural and non-structural) according to the EN 1504-3 standard [30].

Characteristic	Requirements			
	Structural		Non-structural	
	Class R4	Class R3	Class R2	Class R1
Compressive strength	≥45 MPa	≥25 MPa	≥15 MPa	≥10 MPa
Adherence (pull-off)	≥2 MPa	≥1.5 MPa	≥0.8 MPa	≥0.5 MPa
Modulus of elasticity	≥20 GPa	≥15 GPa	No requirement	
Capillary absorption	≤0.5 kg/m^2·h$^{0.5}$			No requirement

Fig. 5 presents the compressive strength evolution of the alkaline mortar (AABM) with respect to the minimum values established for commercial cements (UG type) by the ASTM C1157 standard [77]; 13 MPa to three days of curing, 20 MPa to seven days of curing and 28 MPa to 28 days of curing. This comparison enabled classification of the alkaline binder based on the mechanical performance of the AABM (34.8 MPa at 28 days) as a GU (general use) type cement. The rapid development of compressive strength of the AABM (10.8 MPa–1 day) is an advantage in the field of "*fast repair materials*", commonly used in "*patch repair*" applications that require almost instantaneous adherence to the substrate.
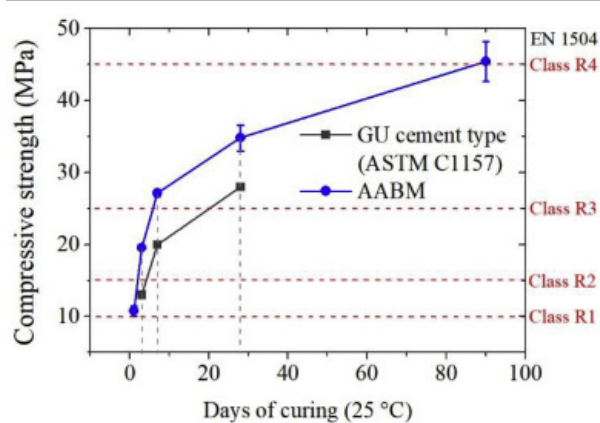
Download high-res image (274KB)   Download full-size image

Fig. 5. Compressive strength evolution of the AABM (cured at room temperature).

The compressive strength of the repair product is an important parameter in applications in which load transfer through the repaired area must be considered. A high-strength concrete that is subjected to high loads must be repaired with a high-strength mortar (≥45 MPa), that is, a mortar of "*class R4*". A low-strength concrete that is subjected to loads must be repaired with a medium-strength structural repair mortar (≥25 MPa), that is, a mortar of "*class R3*". All concretes that are not in a structural situation, that is, situations in which load transfer through the repaired area does not occur, can be repaired with a high-quality non-structural repair mortar (≥15 MPa), that is, a mortar of "*class R2*" [30]. According to the minimum compressive strength requirements (28 days) established by the EN 1504-3 standard [30] for the classification of repair products (Fig. 5), the AABM can be classified as a "*structural repair mortar, class R3*", and attain a value of 34.8 MPa (≫25 MPa). However, the compressive strength is not the only parameter demanded by this classification (Table 4).

Based on previous considerations, some applications (non-structural) do not require an elevated compressive strength by the repair material. A tensile strength of the repair material that is greater than the tensile strength of the substrate favours a "pull-off" failure in the interior of the substrate (ideal situation). Conversely, a tensile strength of the repair material that is less than the tensile strength of the substrate would provoke the cohesive failure of the coating if its adherence to the substrate exceeds its tensile strength. In this case, the EN 1504-3 standard [30] demands a minimum tensile strength of the repair material of 0.5 MPa. Table 5 lists the results obtained for the splitting tensile strength (2.13 MPa) and flexural strength (3.75 MPa) of the AABM, determined at 28 days of curing. These values are consistent with the compressive strength level (Fig. 5) attained by the AABM and exceed the value specified by the EN 1504-3 standard [30].

Table 5. Splitting tensile strength, flexural strength and modulus of elasticity of the AABM (28 days of curing at room temperature).
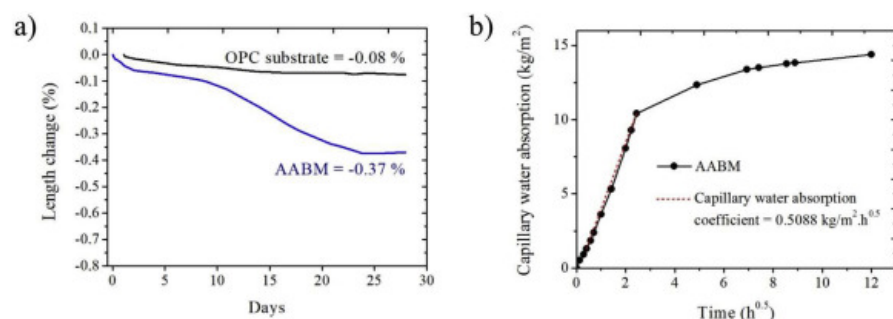
Splitting tensile strength (MPa)	Flexural strength (MPa)	Modulus of elasticity (GPa)
2.13±0.08	3.75±0.47	8.66±0.25

Splitting tensile strength (MPa)	Flexural strength (MPa)	Modulus of elasticity (GPa)

The modulus of elasticity is considered to be an important property as it is related to the rigidity. Significant differences in the modulus of elasticity between the repair material and the substrate can cause premature failure of the repaired area [1]. The AABM attained a modulus of elasticity value of 8.66 GPa at 28 days of curing (Table 5), which coincides with the range (3.8–15 GPa) reported by Kheradmand et al., in 2017 [78] for alkaline mortars. These authors claim that an adjustment in the alkaline activator content, that is, a reduction of the activator/binder ratio at the same time of an increment in the Na_2SiO_3/NaOH ratio causes higher modulus of elasticity values; however, these adjustments also increase the shrinkage level and the cracking susceptibility of the alkaline mortars [29,48,79].

Incompatibilities between the repair mortar and the surface to be repaired can cause premature failure, especially due to the differential shrinkage level [29,80]. This can promote a shear stress between layers that affect the adherence. Fig. 6a shows the shrinkage percentage (–), recorded up to 28 days, of the AABM with respect to the OPC substrate (–0.37% vs. –0.08%, respectively). Even with this shrinkage level (high), note than the coating did not present signs of surface cracking (cracks). According to Kani and Allahverdi (2011) [79], a decrease in the shrinkage is possible with a decrease in the SiO_2/Na_2O, H_2O/Al_2O_3 and/or Na_2O/Al_2O_3 molar ratios; however, some authors [4,31,[81], [82], [83]] have demonstrated that these adjustments affect the mechanical performance and adherence (pull-off) to the substrate. Addition of fibers in the mixture (fibre-reinforced composites) [84,85] can reduce the shrinkage (it depends on many parameters such as fiber length, fiber type, dosage). A shrinkage control parameter is the increment of the precursor:sand ratio. The aggregate (sand) acts as reinforcement in the matrix, that is, an increase of this ratio would provide high-dimensional stability for the material. However, the mechanical performance and adherence level to the substrate may also decrease.

Fig. 6. a) Shrinkage level (ASTM C490 [63]) of AABM vs OPC substrate and b) Capillary water absorption (EN 1015-18 [62]) of the AABM.

In addition to the required mechanical specifications, the exposure conditions to which the material will be subjected are considered important, as these conditions determine the durability of the system. For this reason, the EN 1504-3 standard [30] specifies a capillary absorption coefficient that is less than $0.5\,kg/m^2 \cdot h^{0.5}$ as an acceptable limit of the permeability level for "*class R2, R3 and R4*" repair products. For the case of "*class R1*", no value is specified. According to the results (Fig. 6b), the AABM presents a capillary absorption coefficient of $0.5088\,kg/m^2 \cdot h^{0.5}$, which can be considered as the limit for complying with the specification established by the standard.

3.3. Pull-off test

Fig. 7 shows the results of the pull-off test as a function of the class of concrete substrate (C25/30, C35/45 and C50/60). According to the specifications of the EN 1504-3 standard [30], the adherence of the repair material to the substrate must exceed 1.5 MPa and 2.0 MPa for "*class R3*" and "*class R4*" structural products, respectively, and exceed 0.8 MPa for "*class R1*" and "*class R2*" non-structural products (Table 4). The AABM adherence was 0.75 MPa, 1.14 MPa and 1.24 MPa for the case of substrates with compressive strength of 36.2±2.4, 50.3±2.3 and 64.9±1.7 respectively. This finding indicates that the AABM can be classified as a "*class R2*" repair mortar, with its adherence improved by the quality of the substrate. The pull-off strength must be ≥0.8 MPa for this classification according to the EN 1504-3 standard [30].
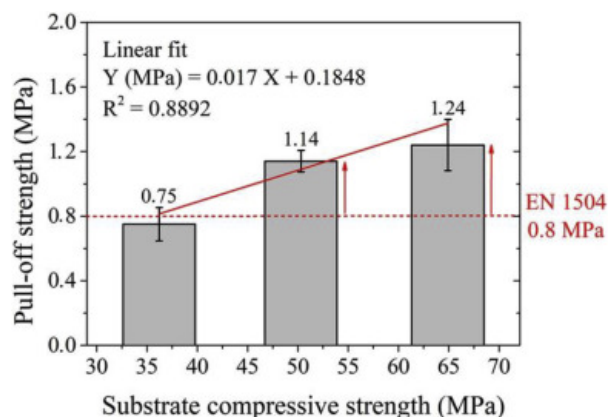
Fig. 7. AABM adherence (pull-off) as a function of substrate class (C25/30, C35/45 and C50/60).

In Fig. 7, it is observed a direct relationship between the mechanical properties of the substrate and the bond strength between the substrate (OPC concrete) and the repair material (AABM). The relationships between these two variables can be expressed with a simple linear regression model, which presented a correlation coefficient $R^2 = 0.89$. Bonaldo et al., 2005 [86] investigated the effect of substrate compressive strength (C16/20, C35/45 and C55/67) on the adhesion strength of several commercially available bond products, in this study pull-off test was also used for measuring the adhesion properties. They conclude that the strength of the substrate plays a major role in the pull-off strength, the relation obtained between the two variables was lineal with $R^2 = 0{,}6995$, value lower than that obtained in the present study using an alkali-activated material. These authors [86] report similar adherence results for OPC concretes using this method (pull-off) and highlight that the strength class of the substrate is related to the porosity of the surface that is in contact with the coating (interface). The lower the substrate strength is, the higher the surface porosity and the tendency towards water absorption, which promotes the formation of a water film during the coating application and affects its adherence.

Excellent adherence is presented by the AAM on the surface of OPC-based concretes; according to Pacheco-Torgal et al. (2008) [34], as the surface of the OPC substrate is rich in calcium hydroxide ($Ca(OH)_2$), which reacts with the alkaline binder due to the need for positive ions, such as Ca^{++}, that are capable of balancing the negative charge of the Al^{3+} during the formation of the geopolymeric structure. Thus, the adherence between both materials also exhibits chemical characteristics. Some authors claim that the adherence of the AAM is improved by a high content of alkaline activator (SiO_2/Al_2O_3 ratio) [4,31,[81], [82], [83]], especially silicates (Na_2SiO_3 o K_2SiO_3). However, this practice causes significant shrinkage [3] and a high cracking susceptibility of the coating, which is not desirable for this type of application.

According to the EN 1542 standard classification presented in Table 6 [65], there is different modes of failure for pull-off tests. The failure can occur at the concrete substrate, at the repair overlay material, at the bond interface, or at the epoxy or adhesive used to bond the two materials. If the failure occurs partially in two different modes is considered as a combination of the failure modes. In the present study the pull-off failure of the AABM for the three classes of substrate (C25/30, C35/45 and C50/60) corresponds to the combination of an A/B-type adhesive failure and a B-type cohesive failure (Fig. 8). Given the absence of B/C-type failures, the cohesive rupture of the coating is discarded, which indicates that the tensile strength of the AABM (2.13 MPa) was not exceeded by the maximum load during the pull-off test (0.75–1.24 MPa). The strength of the OPC substrates, although they favoured the adherence, did not influence the type of failure as the force did not exceed the tensile strength of the OPC substrates in any of the cases.

Table 6. Type of failure classification after the pull-off test (EN 1542) [65].

Type of failure	Descriptions
A	Cohesion failure in the concrete substrate (ideal)
A/B	Adhesion failure between the substrate and the first layer (ideal)
B	Cohesion failure in the first layer
B/C	Adhesion failure between the first and second layer
C	Cohesion failure in the second layer
-/Y	Adhesion failure between the last layer and adhesive layer (abnormal)
Y	Cohesion failure in the adhesive layer (abnormal)
Y/Z	Adhesion failure between the adhesive layer and the dolly (abnormal)
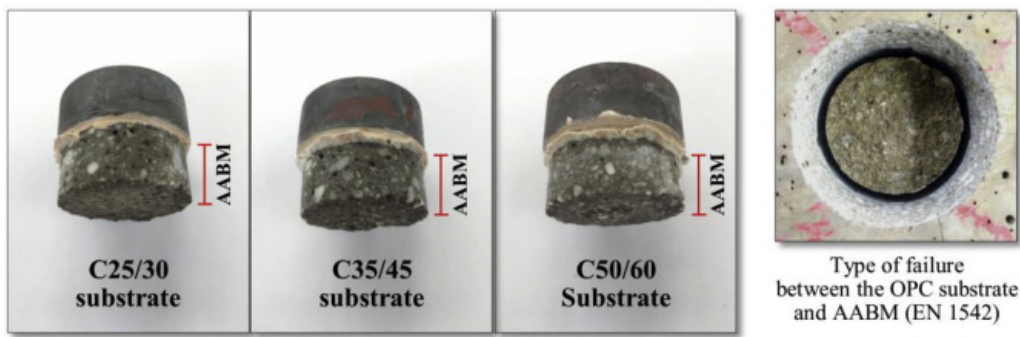
Download high-res image (405KB)   Download full-size image

Fig. 8. Visual determination of the type of failure (pull-off test) (EN 1542).

4. Conclusions

In this study was evaluated the potential of an alkali-activated binary mortar (AABM), based on a natural volcanic pozzolan (70%) and granulated blast furnace slag (30%), as a repair material. Physical and mechanical properties were investigated. According the results obtained, it is possible conclude:

- The compressive strength of the AABM (34.8 MPa at 28 days) would enable its classification as a *"structural repair mortar, class R3"*. However, the modulus of elasticity values (8.66 GPa) must be increased beyond 15–20 GPa, and the adherence (0.75–1.24 MPa) must be increased to values above 1.5–2.0 MPa, using other formulations.

- The results of the pull-off test demonstrate the adherent nature of the AABM, which was promoted by the strength (quality) of the OPC substrate, with pull-off adherences of 0.75 MPa, 1.14 MPa and 1.24 MPa for the cases of C25/30, C35/45 and C50/60, respectively. This aspect is relevant and should be evaluated in conjunction with the increased quality of the alkali-activated coating using other formulations in the search of *"class R3 and R4"* structural classifications.

- The differential shrinkage between the substrate and the repair product can be an incompatibility between both materials. The shrinkage level of the AABM was significantly higher than the shrinkage level of the OPC substrate (–0.37% vs. –0.08%, respectively). Even when no cracking phenomena were observed in these conditions, its reduction is recommended using other formulations and/or incorporating short fibres (fiber-reinforced composites).

Finally, according to the characterisation of the AABM and the specification of the EN 1504-3 standard regarding compressive strength, splitting tensile strength, adherence (pull-off), modulus of elasticity and capillary absorption, this material can be classified as a *"non-structural repair mortar, class R2"*, which is suitable for use in the repair of structures that do not have to transfer loads through the repaired area. Additional aspects of this classification, which are associated with the use of this material as a repair or surface protection (coating) system to promote a high durability (or chemical resistance) in concrete structures subjected to severe conditions (CO_2, chloride, sulphates, acids, fire, etc.), are considered of interest for subsequent studies.

Acknowledgements

Recommended articles   Citing articles (0)

References

[1]   F. Pacheco-Torgal, Z. Abdollahnejad, S. Miraldo, S. Baklouti, Y. Ding
An overview on the potential of geopolymers for concrete infrastructure rehabilitation
Constr. Build. Mater., 36 (2012), pp. 1053-1058, 10.1016/j.conbuildmat.2012.07.003
Article   Download PDF   View Record in Scopus   Google Scholar

[2]   A.Z.W. Wazien, M. Mustafa, A. Bakri, R.A. Razak, M.A.Z.R. Rozainy, M. Faheem, M. Tahir, M.A. Faris
Review on potential of geopolymer for concrete repair and rehabilitation
MATEC Web Conf (2016), p. 01065, 10.1051/matecconf/20167801065

6–11

Google Scholar

[3] G. Fahim Huseien, J. Mirza, M. Ismail, S.K. Ghoshal, A. Abdulameer Hussein
Geopolymer mortars as sustainable repair material: a comprehensive review
Renew. Sustain. Energy Rev., 80 (2017), pp. 54-74, 10.1016/j.rser.2017.05.076
Article   Download PDF   View Record in Scopus   Google Scholar

[4] S. Kramar, A. Šajna, V. Ducman
Assessment of alkali activated mortars based on different precursors with regard to their suitability for concrete repair
Constr. Build. Mater., 124 (2016), pp. 937-944, 10.1016/j.conbuildmat.2016.08.018
Article   Download PDF   View Record in Scopus   Google Scholar

[5] S. Hu, H. Wang, G. Zhang, Q. Ding
Bonding and abrasion resistance of geopolymeric repair material made with steel slag
Cement Concr. Compos., 30 (2008), pp. 239-244, 10.1016/J.CEMCONCOMP.2007.04.004
Article   Download PDF   CrossRef   View Record in Scopus   Google Scholar

[6] K. Pavel, P. Oleg, V. Hryhorii, L. Serhii
The development of alkali-activated cement mixtures for fast rehabilitation and strengthening of concrete structures
Procedia Eng, 195 (2017), pp. 142-146, 10.1016/j.proeng.2017.04.536
Article   Download PDF   View Record in Scopus   Google Scholar

[7] V. Ducman, S. Kramar, A. Šajna
11 – alkali activated repair mortars based on different precursors
Eco-Efficient Repair Rehabil. Concr. Infrastructures (2018), pp. 263-292, 10.1016/B978-0-08-102181-1.00011-3
Article   Download PDF   View Record in Scopus   Google Scholar

[8] L.K. Turner, F.G. Collins
Carbon dioxide equivalent (CO2-e) emissions: a comparison between geopolymer and OPC cement concrete
Constr. Build. Mater., 43 (2013), pp. 125-130, 10.1016/j.conbuildmat.2013.01.023
Article   Download PDF   View Record in Scopus   Google Scholar

[9] B.C. McLellan, R.P. Williams, J. Lay, A. Van Riessen, G.D. Corder
Costs and carbon emissions for geopolymer pastes in comparison to ordinary portland cement
J. Clean. Prod., 19 (2011), pp. 1080-1090, 10.1016/j.jclepro.2011.02.010
Article   Download PDF   View Record in Scopus   Google Scholar

[10] G. Habert, J.B. D'Espinose De Lacaillerie, N. Roussel
An environmental evaluation of geopolymer based concrete production: reviewing current research trends
J. Clean. Prod., 19 (2011), pp. 1229-1238, 10.1016/j.jclepro.2011.03.012
Article   Download PDF   View Record in Scopus   Google Scholar

[11] P. Duxson, J.L. Provis
Designing precursors for geopolymer cements
J. Am. Ceram. Soc., 91 (2008), pp. 3864-3869, 10.1111/j.1551-2916.2008.02787.x
CrossRef   View Record in Scopus   Google Scholar

[12] J.L. Provis, S.A. Bernal
Geopolymers and related alkali-activated materials
Annu. Rev. Mater. Res., 44 (2014), pp. 299-330, 10.1146/annurev-matsci-070813-113515
CrossRef   View Record in Scopus   Google Scholar

[13] A. Palomo, P. Krivenko, I. Garcia-Lodeiro, E. Kavalerova, O. Maltseva, A. Fernández-Jiménez
A review on alkaline activation: new analytical perspectives
Mater. Construcción, 64 (2014), p. e022, 10.3989/mc.2014.00314
CrossRef   Google Scholar

[14] F. Pacheco-Torgal, J. Castro-Gomes, S. Jalali
Alkali-activated binders: a review. Part 1. Historical background, terminology, reaction mechanisms and hydration products
Constr. Build. Mater., 22 (2008), pp. 1305-1314, 10.1016/j.conbuildmat.2007.10.015
Article   Download PDF   View Record in Scopus   Google Scholar

[15] P. Krivenko

Why alkaline activation – 60 years of the theory and practice of alkali-activated materials

J. Ceram. Sci. Technol. (2017), pp. 323-334, 10.4416/JCST2017-00042

View Record in Scopus   Google Scholar

[16] R. Çetintaş, S. Soyer-Uzun

Relations between structural characteristics and compressive strength in volcanic ash based one–part geopolymer systems

J. Build. Eng., 20 (2018), pp. 130-136, 10.1016/j.jobe.2018.07.011

Article   Download PDF   View Record in Scopus   Google Scholar

[17] Z.N.M. Ngouloure, B. Nait-Ali, S. Zekeng, E. Kamseu, U.C. Melo, D. Smith, C. Leonelli

Recycled natural wastes in metakaolin based porous geopolymers for insulating applications

J. Build. Eng., 3 (2015), pp. 58-69, 10.1016/j.jobe.2015.06.006

Article   Download PDF   View Record in Scopus   Google Scholar

[18] J. Davidovits

Geopolymers - inorganic polymeric new materials

J. Therm. Anal., 37 (1991), pp. 1633-1656, 10.1007/BF01912193

CrossRef   View Record in Scopus   Google Scholar

[19] V.K. Nagaraj, D.L. Venkatesh Babu

Assessing the performance of molarity and alkaline activator ratio on engineering properties of self-compacting alkaline activated concrete at ambient temperature

J. Build. Eng., 20 (2018), pp. 137-155, 10.1016/j.jobe.2018.07.005

Google Scholar

[20] F. Puertas

Cementos de escorias activadas alcalinamente: situación actual y perspectivas de futuro

Mater. Constr., 45 (1995), pp. 53-64, 10.3989/mc.1995.v45.i239.553

CrossRef   View Record in Scopus   Google Scholar

[21] A. Fernández-Jiménez, F. Puertas, I. Sobrados, J. Sanz

Structure of calcium silicate hydrates formed in alkaline-activated slag: influence of the type of alkaline activator

J. Am. Ceram. Soc., 86 (2003), pp. 1389-1394, 10.1111/j.1151-2916.2003.tb03481.x

CrossRef   View Record in Scopus   Google Scholar

[22] I. Garcia-Lodeiro, A. Palomo, A. Fernández-Jiménez, D.E. MacPhee

Compatibility studies between N-A-S-H and C-A-S-H gels. Study in the ternary diagram Na2O-CaO-Al2O3-SiO2-H2O

Cement Concr. Res., 41 (2011), pp. 923-931, 10.1016/j.cemconres.2011.05.006

Article   Download PDF   View Record in Scopus   Google Scholar

[23] I. García-Lodeiro, A. Fernández-Jiménez, M.T. Blanco, A. Palomo

FTIR study of the sol-gel synthesis of cementitious gels: C-S-H and N-A-S-H

J. Sol. Gel Sci. Technol., 45 (2008), pp. 63-72, 10.1007/s10971-007-1643-6

CrossRef   View Record in Scopus   Google Scholar

[24] J.L. Provis, A. Palomo, C. Shi

Advances in understanding alkali-activated materials

Cement Concr. Res., 78 (2015), pp. 110-125, 10.1016/j.cemconres.2015.04.013

Article   Download PDF   View Record in Scopus   Google Scholar

[25] C. Shi, A.F. Jiménez, A. Palomo

New cements for the 21st century: the pursuit of an alternative to Portland cement

Cement Concr. Res., 41 (2011), pp. 750-763, 10.1016/j.cemconres.2011.03.016

Article   Download PDF   View Record in Scopus   Google Scholar

[26] J.S.J. Van Deventer, J.L. Provis, P. Duxson

Technical and commercial progress in the adoption of geopolymer cement

Miner. Eng., 29 (2012), pp. 89-104, 10.1016/j.mineng.2011.09.009

Article   Download PDF   View Record in Scopus   Google Scholar

[27] D.M. Roy

Alkali-activated cements: opportunities and challenges
Cement Concr. Res., 29 (1999), pp. 249-254, 10.1016/S0008-8846(98)00093-3
Article   🔝 Download PDF   View Record in Scopus   Google Scholar

[28]   L. Song, Z. Li, P. Duan, M. Huang, X. Hao, Y. Yu
Novel low cost and durable rapid-repair material derived from industrial and agricultural by-products
Ceram. Int., 43 (2017), pp. 14511-14516, 10.1016/j.ceramint.2017.07.106
Article   🔝 Download PDF   View Record in Scopus   Google Scholar

[29]   E. Vasconcelos, S. Fernandes, J.L. Barroso Aguiar, F. Pacheco-Torgal
Concrete retrofitting using metakaolin geopolymer mortars and CFRP
Constr. Build. Mater., 25 (2011), pp. 3213-3221, 10.1016/j.conbuildmat.2011.03.006
Article   🔝 Download PDF   View Record in Scopus   Google Scholar

[30]   European Standard, EN 1504
Products and Systems for the Protection and Repair of Concrete structures. Part 3: Structural and Non-structural Repair
(2005)
Google Scholar

[31]   T. Phoo-ngernkham, A. Maegawa, N. Mishima, S. Hatanaka, P. Chindaprasirt
Effects of sodium hydroxide and sodium silicate solutions on compressive and shear bond strengths of FA – GBFS geopolymer
Constr. Build. Mater., 91 (2015), pp. 1-8, 10.1016/j.conbuildmat.2015.05.001
Article   🔝 Download PDF   View Record in Scopus   Google Scholar

[32]   H. Alanazi, M. Yang, D. Zhang, Z. Gao
Bond strength of PCC pavement repairs using metakaolin-based geopolymer mortar
Cement Concr. Compos., 65 (2016), pp. 75-82, 10.1016/j.cemconcomp.2015.10.009
Article   🔝 Download PDF   View Record in Scopus   Google Scholar

[33]   C. Zanotti, P.H.R. Borges, A. Bhutta, N. Banthia
Bond strength between concrete substrate and metakaolin geopolymer repair mortar: effect of curing regime and PVA fiber reinforcement
Cement Concr. Compos., 80 (2017), pp. 307-316, 10.1016/j.cemconcomp.2016.12.014
Article   🔝 Download PDF   View Record in Scopus   Google Scholar

[34]   F. Pacheco-Torgal, J.P. Castro-Gomes, S. Jalali
Adhesion characterization of tungsten mine waste geopolymeric binder. Influence of OPC concrete substrate surface treatment
Constr. Build. Mater., 22 (2008), pp. 154-161, 10.1016/j.conbuildmat.2006.10.005
Article   🔝 Download PDF   View Record in Scopus   Google Scholar

[35]   S.M. Laska, S. Talukdar
Preparation and tests for workability, compressive and bond strength of ultra-fine slag based geopolymer as concrete repairing agent
Constr. Build. Mater., 154 (2017), pp. 176-190, 10.1016/J.CONBUILDMAT.2017.07.187
Google Scholar

[36]   A. Fernandez-Jimenez, I. García-Lodeiro, A. Palomo
Durability of alkali-activated fly ash cementitious materials
J. Mater. Sci., 42 (2007), pp. 3055-3065, 10.1007/s10853-006-0584-8
CrossRef   View Record in Scopus   Google Scholar

[37]   F. Pacheco-Torgal, Z. Abdollahnejad, A.F. Camões, M. Jamshidi, Y. Ding
Durability of alkali-activated binders: a clear advantage over Portland cement or an unproven issue?
Constr. Build. Mater., 30 (2012), pp. 400-405, 10.1016/j.conbuildmat.2011.12.017
Article   🔝 Download PDF   View Record in Scopus   Google Scholar

[38]   S.A. Bernal, J.L. Provis
Durability of alkali-activated materials: progress and perspectives
J. Am. Ceram. Soc., 97 (2014), pp. 997-1008, 10.1111/jace.12831
CrossRef   View Record in Scopus   Google Scholar

[39]   M.M. Hossain, M.R. Karim, M.K. Hossain, M.N. Islam, M.F.M. Zain
Durability of mortar and concrete containing alkali-activated binder with pozzolans: a review

Constr. Build. Mater., 93 (2015), pp. 95-109, 10.1016/j.conbuildmat.2015.05.094

Article   Download PDF   View Record in Scopus   Google Scholar

[40] J. Zhang, C. Shi, Z. Zhang, Z. Ou
Durability of alkali-activated materials in aggressive environments: a review on recent studies
Constr. Build. Mater., 152 (2017), pp. 598-613, 10.1016/j.conbuildmat.2017.07.027

Article   Download PDF   View Record in Scopus   Google Scholar

[41] A. Fernández-Jiménez, A. Palomo
Chemical durability of geopolymers
Geopolymers (2009), pp. 167-193, 10.1533/9781845696382.2.167

Article   Download PDF   CrossRef   View Record in Scopus   Google Scholar

[42] W. Tahri, Z. Abdollahnejad, J. Mendes, F. Pacheco-torgal, J. Barroso de Aguiar
Performance of a fly ash geopolymeric mortar for coating of ordinary portland cement concrete exposed to harsh chemical environments
Adv. Mater. Res., 1129 (2015), pp. 573-580, 10.4028/www.scientific.net/AMR.1129.573

CrossRef   View Record in Scopus   Google Scholar

[43] W. Tahri, Z. Abdollahnejad, J. Mendes, F. Pacheco-Torgal, J.B. de Aguiar
Cost efficiency and resistance to chemical attack of a fly ash geopolymeric mortar versus epoxy resin and acrylic paint coatings
Eur. J. Environ. Civ. Eng., 21 (2017), pp. 555-571, 10.1080/19648189.2015.1134674

CrossRef   View Record in Scopus   Google Scholar

[44] M.H. Al-Majidi, A.P. Lampropoulos, A.B. Cundy, O.T. Tsioulou, S. Al-Rekabi
A novel corrosion resistant repair technique for existing reinforced concrete (RC) elements using polyvinyl alcohol fibre reinforced geopolymer concrete (PVAFRGC)
Constr. Build. Mater., 164 (2018), pp. 603-619, 10.1016/j.conbuildmat.2017.12.213

Article   Download PDF   View Record in Scopus   Google Scholar

[45] A.M. Aguirre-Guerrero, R. Mejía de Gutiérrez
Assessment of corrosion protection methods for reinforced concrete
Eco-Efficient Repair Rehabil. Concr. Infrastructures (2018), pp. 315-353, 10.1016/B978-0-08-102181-1.00013-7

Article   Download PDF   View Record in Scopus   Google Scholar

[46] Z. Zhang, X. Yao, Z. Huajun
Potential application of geopolymers as protection coatings for marine concrete: I. Basic properties
Appl. Clay Sci., 49 (2010), pp. 1-6, 10.1016/J.CLAY.2010.01.014

Article   Download PDF   CrossRef   View Record in Scopus   Google Scholar

[47] Z. Zhang, X. Yao, H. Zhu
Potential application of geopolymers as protection coatings for marine concrete: II. Microstructure and anticorrosion mechanism
Appl. Clay Sci., 49 (2010), pp. 7-12, 10.1016/j.clay.2010.04.024

Article   Download PDF   View Record in Scopus   Google Scholar

[48] Z. Zhang, X. Yao, H. Wang
Potential application of geopolymers as protection coatings for marine concrete: III. Field experiment
Appl. Clay Sci. (2012), pp. 57-60, 10.1016/j.clay.2012.05.008
67–68

Article   Download PDF   View Record in Scopus   Google Scholar

[49] A.M. Aguirre-Guerrero, R.A. Robayo-Salazar, R.M. de Gutiérrez
A novel geopolymer application: coatings to protect reinforced concrete against corrosion
Appl. Clay Sci., 135 (2017), pp. 437-446, 10.1016/j.clay.2016.10.029

Article   Download PDF   View Record in Scopus   Google Scholar

[50] W.M. Kriven, M. Gordon, B.L. Ervin, H. Reis
Corrosion protection assessment of concrete reinforcing bars with a geopolymer coating
Ceram. Eng. Sci. Proc. (2008), 10.1002/9780470339749

Google Scholar

[51] H. Rostami, F. Tovia, R. Masoodi, M. Bahadory

Reduction of corrosion of reinforcing steel in concrete using alkali ash material

J. Solid Waste Technol. Manag., 41 (2015), 10.5276/JSWTM.2015.136

Google Scholar

[52]   A.G. De La Torre, S. Bruque, M.A.G. Aranda

Rietveld quantitative amorphous content analysis

J. Appl. Crystallogr., 34 (2001), pp. 196-202, 10.1107/S0021889801002485

CrossRef   View Record in Scopus   Google Scholar

[53]   J.L. Provis

Alkali-activated materials

Cement Concr. Res. (2016), 10.1016/j.cemconres.2017.02.009

in press

Google Scholar

[54]   R.A. Robayo-Salazar, R. Mejía de Gutiérrez

Natural volcanic pozzolans as an available raw material for alkali-activated materials in the foreseeable future: a review

Constr. Build. Mater., 189 (2018), pp. 109-118, 10.1016/j.conbuildmat.2018.08.174

Article   🗎 Download PDF   View Record in Scopus   Google Scholar

[55]   A. Allahverdi, E.N. Kani, M. Yazdanipour

Effects of blast furnance slag on natural pozzolan- based geopolymer cement

Ceramics-Silickáty., 55 (2011), pp. 68-78

View Record in Scopus   Google Scholar

[56]   R.A. Robayo-Salazar, R. Mejía De Gutiérrez, M. Gordillo

Natural pozzolan-and granulated blast furnace slag-based binary geopolymers

Mater. Constr., 66 (2016), p. e077, 10.3989/mc.2016.03615

Google Scholar

[57]   R.A. Robayo-Salazar, R. Mejia de Gutierrez, F. Puertas

Study of synergy between a natural volcanic pozzolan and a granulated blast furnace slag in the production of geopolymeric pastes and mortars

Constr. Build. Mater., 157 (2017), pp. 151-160, 10.1016/j.conbuildmat.2017.09.092

Article   🗎 Download PDF   View Record in Scopus   Google Scholar

[58]   ASTM International, ASTM C109-16

Standard Test Method for Compressive Strength of Hydraulic Cement Mortars (Using 2-in. or [50-mm] Cusbe Specimens)

(2016)

Google Scholar

[59]   UNE, EN 12390-13:2014

Testing Hardened Concrete - Part 13: Determination of Secant Modulus of Elasticity in Compression

(2014)

Google Scholar

[60]   ASTM International, ASTM C348-14

Standard Test Method for Flexural Strength of Hydraulic-Cement Mortars

(2014)

Google Scholar

[61]   ASTM International, ASTM C496-17

Standard Test Method for Splitting Tensile Strength of Cylindrical Concrete Specimens

(2017), 10.1520/C0496

Google Scholar

[62]   UNE, EN 1015-18:2003

Methods of Test for Mortar for Masonry - Part 18: Determination of Water Absorption Coefficient Due to Capillary Action of Hardened Mortar

(2003)

Google Scholar

[63] ASTM International, ASTM C490-17
Standard Practice for Use of Apparatus for the Determination of Length Change of Hardened Cement Paste, Mortar, and Concrete
(2017)
Google Scholar

[64] UNE, EN 206-1:2008
Concrete - Part 1: Specification, Performance, Production and Conformity
(2008)
Google Scholar

[65] European Standard, EN 1542
Products and Systems for the Protection and Repair of Concrete Structures - Test Methods - Measurement of Bond Strength by Pull-Off
(1999)
Google Scholar

[66] International Organization for Standardization
ISO 13473-1:1997 - Characterization of Pavement Texture by Use of Surface Profiles - Part 1: Determination of Mean Profile Depth
(1997)
Google Scholar

[67] ASTM International, ASTM C1437-15
Standard Test Method for Flow of Hydraulic Cement Mortar
(2015)
Google Scholar

[68] F. Puertas, M. Palacios, H. Manzano, J.S. Dolado, A. Rico, J. Rodríguez
A model for the C-A-S-H gel formed in alkali-activated slag cements
J. Eur. Ceram. Soc., 31 (2011), pp. 2043-2056, 10.1016/j.jeurceramsoc.2011.04.036
Article　📄 Download PDF　View Record in Scopus　Google Scholar

[69] M. Torres-Carrasco, F. Puertas
Alkaline activation of aluminosilicates as an alternative to portland Cement: a review
Rom. J. Mater., 47 (2017), pp. 3-15
View Record in Scopus　Google Scholar

[70] I. Garcia-Lodeiro, S. Donatello, A. Fernández-Jiménez, Á. Palomo
Hydration of hybrid alkaline cement containing a very large proportion of fly ash: a descriptive model
Materials, 9 (2016), 10.3390/MA9070605
Google Scholar

[71] I. García-Lodeiro, A. Fernández-Jiménez, A. Palomo
Variation in hybrid cements over time. Alkaline activation of fly ash-portland cement blends
Cement Concr. Res., 52 (2013), pp. 112-122, 10.1016/j.cemconres.2013.03.022
Article　📄 Download PDF　View Record in Scopus　Google Scholar

[72] M.J. Sánchez-Herrero, A. Fernández-Jiménez, Á. Palomo, L. Klein
Alkaline hydration of C2S and C3S
J. Am. Ceram. Soc., 99 (2016), pp. 604-611, 10.1111/jace.13985
CrossRef　View Record in Scopus　Google Scholar

[73] J.N.Y. Djobo, H.K. Tchakoute, N. Ranjbar, A. Elimbi, L.N. Tchadjie, D. Njopwouo, J. Biernacki
Gel composition and strength properties of alkali-activated oyster shell-volcanic ash: effect of synthesis conditions
J. Am. Ceram. Soc., 99 (2016), pp. 3159-3166, 10.1111/jace.14332
CrossRef　View Record in Scopus　Google Scholar

[74] I. García Lodeiro, D.E. Macphee, A. Palomo, A. Fernández-Jiménez
Effect of alkalis on fresh C-S-H gels. FTIR analysis
Cement Concr. Res., 39 (2009), pp. 147-153, 10.1016/j.cemconres.2009.01.003
Article　📄 Download PDF　View Record in Scopus　Google Scholar

[75] E.N. Kani, A. Allahverdi, J.L. Provis

Efflorescence control in geopolymer binders based on natural pozzolan

Cement Concr. Compos., 34 (2012), pp. 25-33, 10.1016/j.cemconcomp.2011.07.007

Google Scholar

[76]   M. Jafari Nadoushan, A.A. Ramezanianpour

The effect of type and concentration of activators on flowability and compressive strength of natural pozzolan and slag-based geopolymers

Constr. Build. Mater., 111 (2016), pp. 337-347, 10.1016/j.conbuildmat.2016.02.086

Article   PDF Download PDF   View Record in Scopus   Google Scholar

[77]   ASTM International, ASTM C1157-17

Standard Performance Specification for Hydraulic Cement

(2017), 10.1520/C1157

Google Scholar

[78]   M. Kheradmand, Z. Abdollahnejad, F. Pacheco-Torgal

Shrinkage performance of fly ash alkali-activated cement based binder mortars

KSCE J. Civ. Eng., 00 (2017), pp. 1-11, 10.1007/s12205-017-1714-3

CrossRef   Google Scholar

[79]   E.N. Kani, A. Allahverdi

Investigating shrinkage changes of natural pozzolan based geopolymer cement paste, Iran

J. Mater. Sci. Eng., 8 (2011), pp. 50-60

View Record in Scopus   Google Scholar

[80]   D. Cusson

Durability of repaired concrete structures

Fail. Distress Repair Concr. Struct. (2009), pp. 296-321, 10.1533/9781845697037.2.296

Article   PDF Download PDF   CrossRef   View Record in Scopus   Google Scholar

[81]   M. Irfan Khan, K. Azizi, S. Sufian, Z. Man

Effect of Na/Al and Si/Al ratios on adhesion strength of geopolymers as coating material

Appl. Mech. Mater., 625 (2014), pp. 85-89, 10.4028/www.scientific.net/AMM 625.85

CrossRef   View Record in Scopus   Google Scholar

[82]   T. Phoo-ngernkham, V. Sata, S. Hanjitsuwan, C. Ridtirud, Shigemitsu Hatanaka, Prinya Chindaprasirt

High calcium fly ash geopolymer mortar containing Portland cement for use as repair material

Constr. Build. Mater., 98 (2015), pp. 482-488

https://doi.org/10.1016/j.conbuildmat.2015.08.139

Article   PDF Download PDF   View Record in Scopus   Google Scholar

[83]   H.Y. Zhang, V. Kodur, S.L. Qi, B. Wu

Characterizing the bond strength of geopolymers at ambient and elevated temperatures

Cement Concr. Compos., 58 (2015), pp. 40-49, 10.1016/j.cemconcomp.2015.01.006

Article   PDF Download PDF   View Record in Scopus   Google Scholar

[84]   J. Zhang, V.C. Li

Influences of fibers on drying shrinkage of fiber-reinforced cementitious composite

J. Eng. Mech., 127 (2001), pp. 37-44, 10.1061/(ASCE)0733-9399(2001)127:1(37)

CrossRef   View Record in Scopus   Google Scholar

[85]   J.Y. Wang, N. Banthia, M.H. Zhang

Effect of shrinkage reducing admixture on flexural behaviors of fiber reinforced cementitious composites

Cement Concr. Compos., 34 (2012), pp. 443-450, 10.1016/j.cemconcomp.2011.12.004

Article   PDF Download PDF   CrossRef   View Record in Scopus   Google Scholar

[86]   E. Bonaldo, J.A.O. Barros, P.B. Lourenço

Bond characterization between concrete substrate and repairing SFRC using pull-off testing

Int. J. Adhesion Adhes., 25 (2005), pp. 463-474, 10.1016/j.ijadhadh.2005.01.002

Article   PDF Download PDF   View Record in Scopus   Google Scholar

ELSEVIER

About ScienceDirect Remote access Shopping cart Advertise Contact and support Terms and conditions Privacy policy

RELX™